UIVERSITY OF CALIFORNIA

SANTA CRUZ

DENDRITIC SPINE ABNORMALITIES IN A MOUSE MODEL OF FRAGILE X SYNDROME

A thesis submitted in partial satisfaction
of the requirements for the degree of

MASTERS OF ARTS

in

MOLECULAR, CELL AND DEVELOPMENTAL BIOLOGY

by

Adam Aharon

December 2015

The Thesis of Adam Aharon
is approved:

_____
Professor Yi Zuo, Chair

_____
Professor Rohinton Kamakaka

_____
Professor David A. Feldheim

_____
Tyrus Miller
Vice Provost and Dean of Graduate Studies

Table of Contents

List of Figures

Abstract

Adam Aharon

Dendritic spine abnormalities in a mouse model of Fragile X syndrome

Fragile X syndrome (FXS) is the most common form of genetically inherited mental retardation and although it has been investigated for over 20 years, how cognitive function is specifically disrupted remains unknown. One of the most consistent neuronal phenotypes observed in FXS is increased density of dendritic spines, the protrusions that form postsynaptic components of excitatory synapses. This study further investigates spine abnormalities of the mouse model of FXS in different neuronal compartments, cell types, and cortical regions of wild type and mutant mice, as well as heterozygotes. Increased spine density was identified in mutant mice specifically on apical dendrites of layer 5 neurons. This phenotype only manifests during adulthood and the effect is consistent across multiple sensory regions of the cortex. However, effects on spine density differed between neuronal cell types. These findings identify previously unobserved region, cell type, and cell compartment-specific effects in the mouse model of FXS.

To my family and friends

for all of their support and encouragement

Acknowledgments

I would like to first thank my advisor and mentor Dr. Yi Zuo for all of her teaching, support, encouragement and enthusiasm. Her passion and work ethic in the field of neuroscience is unmatched and I feel extremely fortunate to have had the opportunity to learn and grow under her supervision and support. She has given me wonderful opportunities that I would never have had otherwise, and I feel eternally indebted to her for the lessons she bestowed on me in the field of scientific research as well as in life.

I would also like to thank my committee members Rohinton Kamakaka and David Feldheim for their helpful advice and encouragement. Many professors have been very influential to me during my time at UCSC, and working closely with them has greatly taught me what it means to be an effective teacher and mentor. These include, but are not limited to, Susan Strome, Rohinton Kamakaka, Jeremy Lee, Bill Saxton, and Giulia Ruben.

I would like to thank all members of the Zuo lab that I have had the pleasure to work with over the years. In particular I would like to thank Caitlin Moyer for all of her encouragement, support, friendship and helpful criticisms of my work and this thesis. I would also like to thank Eric Chen and Jenifer Hodges for all of their help and friendship, I could not have asked for better lab mates. In addition I would like to thank James Perna for being a constant source of entertaining distraction and good thoughtful and engaging conversation, as well as Anthony Gilmore for his friendship

and humor. I would also like to acknowledge past members of the lab that had a substantial impact on me including Denise Garcia and Xinzhu Yu. Both of whom were instrumental in my development and education, and who both very directly shaped my early experience in research science. I must also thank Forrest Coleman for showing me what a truly high caliber scientist is made of. Throughout my graduate work he continued to be a role model of the type of scientist I hope to become, and who I feel proud to call a friend.

Most of all I would like to thank my loving parents, Cindy and Nahoom Aharon. Their constant support and encouragement throughout my life have been my greatest blessing and I can never thank them enough for all they have done for me. My greatest hope in my life is to make them proud. I love you both very much.

Chapter 1: INTRODUCTION

1.1 Background

1.1.1 Fragile X Syndrome

Fragile X Syndrome (FXS) is widely recognized as the most common form of genetically inherited mental retardation in humans with a prevalence of 1:2,500 to 1:5,000 (Hagerman, 2008; Coffee et al., 2009) and manifests in a spectrum of distinguishing intellectual disabilities and behaviors (Garber et al., 2008; McLennan et al., 2011). As the foremost cause of intellectual disability, FXS lies on the autism spectrum (Hagerman et al., 2010) and approximately half of all patients with FXS meet the criteria for autism diagnosis. The physical characteristics observed in patients with FXS are an elongated face, macroorchidism, large protruding ears as well as chronic ear infection, a propensity for vision and eye disorders, large forehead, low muscle tone, as well as hyper-extensible joints (Hersh and Saul, 2011; Garber et al., 2008). In regard to brain function, individuals with FXS also present intellectual and behavioral impairments such as problems with learning and memory as well as social interaction (Garber et al., 2008; McLennan et al., 2011). In particular, individuals with the disorder have lower than average IQ and suffer from impairments in short-term and working memory, executive function, visual memory and spatial relationships, as well as mathematics and computation (Garber et al., 2008; Hall et al., 2008). Certain behavioral issues are also characteristic of the disorder such as stereotypic movements, social anxiety, hyperactivity, hypersensitivity to sensory stimuli, and increased susceptibility to seizure (Tranfaglia,

2011). At the neuronal level, a hallmark of the disorder is the abundance and increased density of dendritic spines with immature morphologic characteristics (Comery et al., 1997; Galvez and Greenough, 2005; Irwin et al., 2001).

FXS is the result of a mutation in the fragile X mental retardation 1 (*FMR1*) gene located on the X chromosome. The gene was identified in 1991 and was the first known example of a trinucleotide repeat disorder. A CGG trinucleotide repeat in the 5' untranslated region (UTR) of the *FMR1* gene silences expression of its protein product, fragile X mental retardation protein (FMRP) (Verkerk et al., 1991). The *FMR1* gene is located at Xg27.3, and trinucleotide repeats of 200 or more in the UTR preceding it results in the full mutation (loss of all FMRP expression) and leads to the methylation as well as chromatin condensation of the gene, while anywhere from 5-44 CGG repeats is typical for the general population (Hagerman et al., 2010). Although this increase in copy number accounts for the vast majority of cases of FXS, rarely an individual can also be affected by a point mutation within *FMR1* which can result in its silencing (Santoro et al., 2012). The *FMR1* gene is highly conserved across species and the amino acid sequence of the murine ortholog shares 97% homology with human FMRP (Ashley et al., 1993). However, when mice are engineered with the CGG expansion, for unknown reasons the gene does not become methylated and fails to be silenced (Brouwer et al., 2007; Santoro et al., 2012). Therefore, a knockout (KO) mouse model was generated with a deletion in exon 5 of the *Fmr1* gene which results in translational silencing and loss of FMRP expression

(Consorthium et al., 1994). This outcome approximates the full mutation that occurs in FXS patients.

1.1.2 X Chromosome Inactivation

In mammals, sex is determined by the presence or absence of a Y chromosome. Females carry two copies of the X chromosome while males carry one. This presents a unique problem regarding the genes located on sex chromosomes. In females who are heterozygous (HET) for the mutant form of *Fmr1*, each cell contains one wild type (WT) and one KO copy of the gene. As a result of dosage compensation, one of the X chromosomes in females is silenced to balance the expression levels of X chromosome genes to match the dosage of males, who carry only a single copy. In humans, approximately two weeks after fertilization, each cell randomly condenses one of the X chromosomes into a Barr body. This occurs by tightly packaging the DNA into heterochromatin, which makes it inaccessible for transcription, thereby inactivating it. This occurs at the 500-1000 cell stage and the mechanism by which the cell determines which X chromosome is silenced is currently unknown. In contrast, mice go through what is termed "imprinted X inactivation". Starting from the eight cell stage, the paternal X chromosome is preferentially inactivated while the maternal X remains active. Following this, the paternal X is then reactivated in embryonic cells, and random X inactivation occurs at the implantation stage at around day 6.5. Preferential silencing of the paternal X chromosome persists in the extra-embryonic tissues, while random X inactivation

occurs in the embryo proper (Cheng and Disteche, 2004). From these cells, every subsequent daughter cell that results from each division inactivates the same X chromosome as its parent cell. Mouse cortical development and neurogenesis occurs between days E11-18, which is well after the X inactivation fate decision has been made. As a result of this, *Fmr1* HET females will have different populations of neurons within the brain that may or may not be expressing FMRP, and will offer a unique insight and opportunity to investigate what affect this may have.

1.1.3 Fragile X Mental Retardation Protein

FMRP is an RNA binding protein that can be found in all tissues of the body, but is seen at its highest concentrations in the brain and testis (Verkerk et al., 1991; Yuskaitis et al., 2010). It functions as a transcriptional regulator of a number of mRNAs. In neurons, FMRP is thought to function locally in dendrites to help regulate the synthesis of certain proteins (Bassell and Warren, 2008) and also acts as a carrier protein for RNA, thus playing a pivotal role in synaptic development and plasticity by regulating the translation of several other genes (Brown et al., 2001; Chen and Joseph, 2015; Darnell et al., 2011). FMRP represses mRNA transcription of certain genes and results in the loss of their protein products. While it is known that FMRP regulates protein expression by interacting with mRNA, few of the mRNAs that FMRP targets have been fully verified. However, several known target mRNAs relevant to neuronal function include Arc, CamKIIα, Psd95, and Sema3F (Santoro et al., 2012). FMRP has been shown to participate in numerous signaling

pathways, including the metabotropic glutamate receptor (mGluR) pathway, where FMRP is a negative regulator of mGluR stimulated protein synthesis (Bear et al., 2004). mGluR-dependant long-term depression and long-term potentiation play crucial roles in learning and memory (Klein et al., 2015; Iliff et al., 2013; Bear et al., 2004), and an exaggerated response to mGluR stimulation resulting from absence of FMRP may underlie some of the symptoms of FXS. Normally mGluR activity stimulates production of FMRP which acts as a "molecular brake" for certain genes. Because of this, dysfunction in the pathway can result in unregulated transcription of those genes which may contribute to the learning and memory impairments characteristic of FXS. Currently, mGluR antagonists (such as 2-methyl-6-phenylethynyl-pyridine) are undergoing trials as potential therapies, and have actually been shown to alleviate symptoms of FXS such as seizures, dendritic spine abnormalities, as well as several cognitive and behavioral problems (McLennan et al., 2011).

1.1.4 Dendritic Spines

Within the brain, neurons communicate with one another via small connections called synapses. The structure of a synapse is very small (~1μm) and consists of a pre and post synaptic site between which neurons exchange electrochemical signals. Dendritic spines are small postsynaptic membranous protrusions that stud the dendrites of neurons and form connections with presynaptic axonal boutons of other neurons to facilitate this communication. Synapses can be

either excitatory or inhibitory, and dendritic spines are the post-synaptic terminals of the majority of excitatory synapses within the brain. These spines are dynamic structures and exist in a variety of shapes and morphologies. Strong synaptic contacts are typically associated with an increased diameter of the spine head (Bellot et al., 2014), indicating a mature and stable spine that connects to the dendrite via a thin neck. Increased dendritic spine density is often observed in both human patients as well as *Fmr1* KO mice (Comery et al., 1997; Galvez and Greenough, 2005; Irwin et al., 2001) with the majority of the spines exhibiting an immature morphology of a long thin neck with a small head diameter. While immature spine phenotype and increased density are often reported in FXS and in adult *Fmr1* KO mice, there is not a full consensus in developmental timing of the spine phenotype and warrants further investigation (Portera-Cailliau, 2012).

1.1.5 Dendritic Compartments

The different neuronal cell types in the brain generally have specific and distinct morphologies. Different cell types can be identified by their physical characteristics of shape, size, and dendritic branching patterns (Lefebvre et al., 2015). The dendrites of neurons, the processes that extend from the soma and receive signals from the axons of other neurons, have different compartments that can be identified and categorized. The two primary classes of pyramidal neuron dendrites are categorized as apical or basal. Apical dendrites of cortical pyramidal cells are long branches that protrude from the soma toward the pial surface, whereas basal dendrites

branch horizontally from the soma and tend to remain in the relative cortical layer where the cell body resides (**Figure 2b**). Because of these differences in localization, it is likely that apical and basal dendrites of a single cell can contribute to vastly different connections and circuits. For example, it has been observed that layer 5 pyramidal neurons tend to receive more thalamocortical synapses on their basal dendrites compared to their apical segments (Rah et al., 2013). This is important because the functional significance of a synapse is partly determined by its distance from the soma as well as the diameter of the dendrite on which it resides, and apical as well as basal dendrites tend to exhibit dissimilar dendrite diameter and general length. Apical and basal dendrites may also have a dramatically different ratio of excitatory and inhibitory synapses, and could respond to stimuli in dissimilar ways. This has been investigated and confirmed in the hippocampus, and it has been shown that apical and basal processes are not equivalent in their propensity for long-term plasticity (Kaibara and Leung, 1993). Furthermore, changes in dendritic spines themselves have been seen to be affected differentially between apical and basal dendrites in a variety of situations ranging from prenatal nicotine exposure to Alzheimer's disease (Muhammad et al., 2012; Mychasiuk et al., 2013; Steele et al., 2014). Therefore, it is plausible that the loss of FMRP may have differing effects on these distinct neuronal compartments.

1.1.6 Neuronal Circuits

Although it is common and tempting to think of brain dysfunction in terms of problems involving individual cells, this perspective can be quite limited. Indeed, even consideration of isolated regions in the brain can result in a point of view that may be too "zoomed in". Although studying brain function at the synaptic and cellular levels is important for the understanding of a particular disorder or problem, one must inevitably "zoom out" and consider how neurons connect with each other both locally and across multiple brain areas in order to gain a more widespread and systemic view of a disorder. Only by doing this is it possible to gain the knowledge and understanding necessary to potentially target and treat problems involving the entire brain. Investigation of how neural circuits are affected by *Fmr1* silencing will certainly shed new light on the symptoms of FXS.

Abnormal connectivity of neural circuits can lead to impaired learning and memory, as well as social and other behavioral abnormalities, and as a result neural circuits have been studied in various autism spectrum disorders (Isshiki et al., 2014). FXS, being an autism spectrum disorder, could potentially have similar alterations of neuronal circuitry and connectivity. The behavioral symptoms associated with the disorder, such as hyper-sensitivity to sensory stimuli, and susceptibility to epileptic seizures, could be a result of hyper-excitable neural circuits. This could potentially be the consequence of either an increase of excitatory synapses or a decrease of inhibitory synapses within the brain. Investigation of this kind of

excitatory/inhibitory imbalance has begun in autism and some reports demonstrate that lowered IQ and impaired social cognition results from decreased inhibitory signaling and increased excitatory signaling (Cochran et al., 2015).

Synapses formed between specific areas of the brain onto particular cells of the cortex tend to cluster in particular regions of the dendrites and occur on distinctive structures of the cell (Risher et al.; Rah et al., 2013). As a result of this, particular circuits within the brain tend to form more patterned connections onto neuronal architecture, rather than randomly distribute across all regions of a given neuron. An example of this is the distribution and clustering pattern of thalamocortical synapses observed on layer 5 cortical neurons (Rah et al., 2013).

The different neurons of the brain are highly variable in their morphology and architecture. The cortical pyramidal neurons of layer 5 for example, whose primary function is the output of signals from the cortex, possess a characteristic morphology with a somewhat triangular cell body and two distinct types of dendritic compartments: the apical and basal dendritic segments (**Figure 2b**). These differing dendritic structures are likely to participate in varying neuronal circuits.

1.2 Research Objectives

Although FXS has been studied for over two decades, much remains to be understood about the disorder. An understanding of FXS at the cellular, synapse, and circuit level is lacking, and specific knowledge in these areas will lead to more effective therapies and pharmaceuticals that can target the disorder with greater

specificity. Studies of FXS thus far have investigated abnormalities of dendritic spines, but the majority limit their attention to apical dendrites relatively close to the pial surface and focus exclusively on *Fmr1* KOs and WT controls, while failing to consider heterozygous females. Furthermore, all slice and tracing studies of FXS thus far have been done using Golgi staining, which is a potentially biased staining method for investigation of this disorder as the spine density increase could be a histological artifact of fixation and the Golgi method (Portera-Cailliau, 2012).

This study was designed to more thoroughly investigate the dendritic spine abnormalities of FXS, using a different methodology than previous studies, with the goal of elucidating the neuronal alterations observed in the brains of individuals suffering from FXS. I propose that abnormalities seen in FXS involve specific neural circuits rather than individual cells in isolation. As such, I hypothesize that these defects are limited specifically to apical dendrites, as well as particular cell types within the brains of affected individuals. Additionally, I investigate the developmental time in which the abnormal spine density emerges and hypothesise the defect to appear only once adulthood is reached. Analysis of both basal and apical dendrites in multiple brain regions in addition to different cell types was performed to elucidate the specificity of the abnormal spine density phenotype seen in FXS. Unlike previous studies, I not only consider *Fmr1* KO animals and WTs, but also include heterozygous females. To my knowledge, this will be the first study to date to take such an approach to scrutinize these issues from multiple angles and the result

of this study will advance our understanding of abnormalities of dendritic spines in FXS.

1.3 Motivation

The lack of adequate therapies for individuals suffering from FXS is partly due to our current limited understanding and often conflicting evidence of the specifics of the disease at the cellular level (Portera-Cailliau, 2012). This investigation was designed to address gaps in our knowledge of the disorder so that future treatments may be developed that are better suited to address the neuronal mechanisms underlying specific problems faced by affected individuals. Often times, to investigate and gain knowledge of the workings and function of an intact system or process, one asks what changes occur when something goes wrong and it becomes dysfunctional. By shedding light on these problems in the brains of those affected by FXS, the resulting knowledge will not only aid in the understanding of FXS, but will simultaneously illuminate the general workings involved in basic brain functioning and cognition. The hope and goal of this investigation is that one day the knowledge gleaned here will contribute to more effectively treat this malady and that the many individuals suffering from FXS will be able to lead more fulfilling lives and not feel as limited by this unfortunate disorder.

Chapter 2: METHODS

2.1 Animals

The C57BL/6 *Fmr1* KO mouse line (Consorthium et al., 1994) was obtained from Dr. Steve Warren at Emory University. The C57BL/6 GFP-M line mice (Feng et al., 2000) were obtained from the Jackson Laboratory (Tg(Thy1EGFP)MJrs/J, stock number 007788) and were selected for their relatively sparse expression of GFP. Male WT GFP-M line mice were bred with *Fmr1* HET females to obtain WT and KO male littermates, as well as HET or WT females. In this breeding scheme the male parent is GFP+ while the female is not. This yields approximately 50% GFP+ offspring. Both males and females were used in the WT and KO groups, but because the *Fmr1* gene is located on the X chromosome, male animals cannot be heterozyous and therefore only females were included in the HET cohort. Genotypes for GFP and *Fmr1* were determined by PCR (see below).

All procedures and experiments were conducted in accordance to National Institutes of Health guidelines for animal research and were approved by IACUC of UC Santa Cruz. All animals were kept in standard laboratory housing with food and water available *ad libitum*. For the purpose of delineating the role of FMRP in development, animals were investigated at either postnatal day ~30 (adolescence) or ~120 (adulthood).

2.2 Genotyping

Three *Fmr1* primers were used (Common: CTT CTG GCA CCT CCA GCT T; Wild Type: TGT GAT AGA ATA TGC AGC ATG TGA; Mutant: CAC GAG ACT AGT GAG ACG TG) and four primers for GFP-M line were used (Control forward: CTA GGC CAC AGA ATT GAA AGA TCT; Control reverse: GTA GGT GGA AAT TCT AGC ATC ATC C; Transgene forward: ACA GAC ACA CAC CCA GGA CA; Transgene reverse: CGG TGG TGC AGA TGA ACT T) as obtained from the Jackson Laboratory. Tissue was obtained by ear punch and put into lysis buffer with proteinase k and incubated overnight at 60°C. Samples were then heated for 10 minutes at 100°C and spun down in a centerfuge at 13,200 RPM for 30 seconds. 1µl of sample DNA was mixed with 1µl of each primer in the reaction and 10µl of master mix (GoTaq Hot Start Green Master Mix 2X, Promega) and water for a total volume of 20µl per sample. PCR was performed on a BioRad thermocycler with a denaturation step of 94°C, annealing step of 59°C, and an elongation step of 72°C for 35 cycles. Samples were then run on a 2% agarose gel using electrophoresis.

2.3 Tissue Preparation and Immunohistochemistry

At the appropriate age, animals were anesthetized with an intraperitoneal injection of a mixture of ketamine (20mg/ml) and xylazine (2mg/ml) (0.02ml/g body weight) and transcardial perfusion was performed with 0.01M phosphate buffered saline (PBS) followed by 4% paraformaldahyde (PFA). The brains were immediately removed and post-fixed in 4% PFA overnight, followed by 2 days incubation in a

cryoprotective solution [30% sucrose, 0.05% sodium azide in tris buffered saline (TBS)]. Whole brains were then mounted to a chuck using OCT (optimal cutting temperature, Tissue-Tek) compound and sectioned in the coronal plane on a Leica CM3050-S cryostat at a thickness of 40µm. This thickness was chosen in order to preserve much of the dendritic structure while simultaneously allowing excellent penetration of antibodies for immunohistochemistry (described below). Sections were collected and stored in 0.05% sodium azide in TBS and stored in well plates at 4°C.

Brain slices were immunostained to reveal GFP+ neurons under bright field imaging. Sections were first rinsed three times in TBS (10 minutes each) followed by incubation in blocking solution (10% normal serum in 0.5% Triton X) for one hour at room temperature. Tissue was then incubated in rabbit anti-GFP primary antibody (abcam) at a dilution of 1:5000 overnight at 4° C. Tissue was then put through 3 TBS rinses before incubation in biotinylated goat anti-rabbit secondary antibody at a dilution of 1:400 (Vector Labs) for 1 hour at room temperature. Tissue was rinsed again in TBS three times before incubation in the avidin/biotin-based peroxidase system (VECTASTAIN Elite ABC system, Vector Labs) for one hour at room temperature. Tissue was rinsed again in TBS three times and incubated in DAB (3,3'-diaminobenzidine peroxidase substrate kit, Vector Labs) for approximately 2 minutes. Stained sections were then rinsed three times in TBS before mounting onto glass slides (Colorfrost Plus, Fisher). After brain sections were mounted and allowed to dry, they were dehydrated in ethanol solutions of increasing concentration (50%,

70%, 95%, 100%, 100% EtOH, three minutes each) and were then defatted by submerging two times, three minutes each in 100% Xylene solution before being coverslipped using DPX Mounting Medium (Electron Microscopy Sciences).

Immunofluorescent staining of FMRP was done using a similar protocol starting with three rinses in TBS (10 minutes each) followed by incubation in blocking solution (10% normal serum in 0.5% Triton X) for one hour at room temperature. Tissue was then incubated in rabbit anti-FMRP primary antibody (abcam) at a dilution of 1:1000 overnight at 4° C. Tissue was then put through three rinses of TBS before incubation in AlexaFluor 594 conjugated goat anti-rabbit secondary antibody (Invitrogen) at a dilution of 1:1000 for two hours at room temperature protected from light. Stained tissue sections were then rinsed three more times in TBS prior to mounting. Fluorescently stained tissue was mounted on slides and quickly coverslipped using Fluoromount-G (Southern Biotech).

2.4 Cell Counts

Animals from the GFP-M line have the vast majority of intrinsic GFP expression in cortical layer 5 (L5) pyramidal neurons as well as robust expression in the hippocampus. Tissue from animals was stained with FMRP-targeting primary antibody to assess the protein expression pattern of the differing genotypes. Cell counts were then performed on the L5 pyramidal neurons that express GFP in the barrel field of the somatosensory cortex, and the number of these cells that were also expressing FMRP was determined. Stereo Investigator software (MBF Bioscience

Inc.) was used to mark and quantify cells. GFP+ neurons that showed any FMRP labeling within the perimeter of the cell body, no matter how dim, were counted as FMRP+. WT animals showed very robust and strong labeling of FMRP while the very small number of FMRP+ cells seen in the KOs had labeling that was dramatically dimmer, yet still contained in the body of the cell and as such counted as FMRP+. The experimenter was blind to all genotypes until all analysis was complete.

2.5 Cell Tracing

Stained brain sections were imaged and traced using a Zeiss Axio Imager.M2 microscope with a 63x oil immersion objective lens (NA 1.4), and the contrast was enhanced by differential interference contrast (DIC) microscopy. The microscope was equipped with a digital camera (AxioCam MRc, Zeiss), motorized stage and x-y-z encoder, and the computer dedicated to this microscope was equipped with Neruolucida software (MBF Bioscience Inc.) which was used for tracing dendritic branches and spines. A diverse set of brain regions were chosen for analysis, including: barrel field, primary auditory, and primary visual regions of sensory cortex, as well as the CA1 region of the hippocampus. To assure accuracy of areas investigated, brain regions were identified using a mouse brain atlas (The Mouse Brain in Stereotaxic Coordinates, Second Edition, Academic Press 2001). GFP immunolabeled apical tufts from layer 5 pyramidal neurons were traced from a distance of ~100-150µm below the pial surface to their termination point, and their

basal segments branching directly off the cell body were traced from the soma to their termination point. The small number of dendritic segments in both apical and basal branches ≤2µm in length were omitted from analysis. Similar analysis was performed on L2/3 pyramidal neurons whose cell bodies reside approximately 150-250µm from the pial surface. Apical and basal dendritic segments of CA1 hippocampal neurons of 100 µm or longer were selected for tracing and subsequent analysis. Simple cells of layer 5 were identified under low magnification based on their apical tuft branching pattern, and only the cells with the majority of dendritic branches intact within the section and whose dendrites were sufficiently filled were selected for tracing. Dendritic spines were defined as any visible protrusion on the dendrites of traced segments.

Branch order was obtained from NeuroExplorer data of tracings. First order dendrites of apical tufts of L5 pyramidal neurons represent the first 5-20µm of the main apical shaft, before the main branching of the apical tuft. First order dendrites of basal segments represent the initial segments of dendrite sprouting directly from the soma. Subsequent branch orders increase sequentially after each node of the dendrite (**Figure 3a**).

2.6 Data Analysis

Reconstructed dendritic data were analyzed using NeuroExplorer (MBF Bioscience Inc.) and Microsoft Excel. Spine density was defined as the total number of dendritic spines observed on a given dendrite divided by the total length of the

traced dendrite. Densities of individual dendritic segments from individual cells were calculated and were reported as numerical averages of all cells of all animals of a particular genotype (**Table 1**). Standard deviation and student *t*-test were calculated for all cases. 2 way ANOVA analysis was performed using Statistica (StatSoft).

Chapter 3: RESULTS

3.1 FMRP expression reduced in KO mice

In order to investigate the neuronal abnormalities seen in the *Fmr1* KO mouse model, it is necessary to first determine that the neurons being studied are indeed lacking expression of FMRP. Fluorescent immunohistochemistry was used to visualize FMRP in cortical tissue to determine its presence in neurons.

Animals from the GFP-M line have the vast majority of intrinsic GFP expression in cortical layer 5 (L5) pyramidal neurons. Tissue from animals was stained with FMRP-targeting primary antibody to assess the protein expression pattern of *Fmr1* KO, HET, and WT animals (**Figure 1a**). Cell counts were then performed on the L5 pyramidal neurons in the barrel field of the somatosensory cortex that express GFP, and the number of these cells that were also expressing FMRP was then quantified.

In the WT animals, nearly all GFP-expressing neurons also expressed FMRP (94±2.5%) (**Figure 1b**). In contrast, the *Fmr1* KO animals showed almost no expression of FMRP within the GFP+ neurons (5±2.8%) (**Figure 1b**). This indicates that although FMRP is not completely absent in the KO animals, its expression is greatly reduced, and therefore provides an ideal platform to study the role of FMRP in the abnormalities of synaptic structures.

3.2 Spine density is differentially altered between apical and basal dendrites of layer 5 neurons of *Fmr1* KO mice

To more fully and accurately investigate the dendritic spine abnormalities seen in FXS, analysis was performed on the apical and basal dendrites of neurons of WT and *Fmr1* KO mice to determine if there are differences in spine alterations between the two types of dendritic compartments. To determine if spine phenotypes differed between apical and basal dendrites in 4 month old adult animals advantage was taken of the intrinsic GFP expression in the mice of the GFP-M line and bright field immunohistochemistry was used to amplify the GFP signal in neurons in order to trace the dendrites and spines.

As is the case in most rodents, the whiskers are specialized mechanosensory structures and are one of the primary sense organs of the mouse. The whiskers are topographically represented individually within a region of the somatosensory cortex known as the barrel field. Each specific compartmentalized cortical region associated with a particular whisker is known as a barrel. Attention was first paid to this region to examine the spines and dendrites of these neurons, as this is such an important sensory area of the mouse cortex.

Commonly, the increased spine density seen in FXS is observed in the more superficial layers of the cortex (Comery et al., 1997; Cruz-Martín et al., 2010; Nimchinsky et al., 2001). Thus, first to be examined were the apical tufts of the labeled L5 pyramidal neurons within the barrel field of the somatosensory cortex that

branch out into layer 1. These tufts typically open up around 100-150 µm from the pial surface and run parallel to the pial plane. An increase of dendritic spines in the apical tufts of these layer 5 pyramidal neurons in 4 month old *Fmr1* KO mice was observed (WT 0.6±0.05 spines/µm, KO 0.99±0.04 spines/µm; $p<0.001$). However, the basal dendrites showed no significant difference between genotypes (WT 0.55±0.07 spines/µm, KO 0.54±0.06 spines/µm; $p=0.89$) (**Figure 2d**).

This significant increase in spine density on apical dendrites was further investigated by analysis of branch order in these tufts. The structure of the apical tuft is a pattern of increasing complexity as the dendrites extend away from the primary apical shaft. At each node of bifurcation, the order of the dendritic branch increases by one, where the first order dendrite corresponds to the primary apical shaft (**Figure 3a**). Categorizing the dendritic branches this way allowed more accurate analysis of the regions where this spine density difference between WT and KO mice occurs. Overall, spine density of apical tufts decreased with increasing branch order and this trend was maintained across all genotypes ($p>0.05$). However, spine density was significantly increased in the KO in the first, second and third order dendrites relative to WT (two-way ANOVA: $F(5, 220)=168.37$, $p<0.001$), but not in any subsequent branch orders, nor did they show a difference in the basal dendrites (**Figure 3b**).

3.3 Dendritic spine alterations in somatosensory cortex of *Fmr1* KO mice are consistent across multiple cortical sensory regions

The cerebral cortex is partitioned into separate regions that are responsible for distinct functions. Broadly, the regions of the cortex are characterized into 3 main classes: the sensory, motor, and association areas. Each of these areas is responsible for dealing with specific functions. The motor cortex is primarily responsible for the control of voluntary movements, while sensory cortex processes all of the input from the various sense organs. The sensory cortex is subdivided into the somatosensory cortex, visual cortex, and auditory cortex, which process touch, vision, and audition, respectively. The association cortex generally functions to produce a meaningful experience from perceptual occurrences and is the main area involved in advanced thinking such as abstract thought and language.

Since individuals suffering from FXS are generally hyperactive and hypersensitive to sensory stimuli (Tranfaglia, 2011), it was next asked if the dendritic spine increase observed in FXS and in *Fmr1* KO mice is consistent across different sensory areas of the cerebral cortex besides the barrel field in adult animals (~4 months). The same approach that was employed previously was again used here to label and trace the dendrites and spines of the layer 5 pyramidal cells in these different regions of the adult WT and KO mice to ask if this trend is observable across the various sensory cortices.

Rodents have a well developed auditory cortex, and mice can perceive ultrasonic auditory stimulus well outside of the range of human hearing. Individuals suffering from FXS display hypersensitivity to auditory stimuli and the mouse model of the disorder shows similar abnormalities displayed as increased acoustic startle response, audiogenic seizures, and hyperexcitability of auditory neurons as observed via electrophysiological recording (Dansie et al., 2013; Rotschafer and Razak, 2014, 2013). Using the same tracing methods as for the barrel cortex, attention shifted to the layer 5 cells of four month old adult WT and KO animals to determine if apical spine density is similarly altered in the auditory cortex.

Similar to the barrel field, layer 5 cortical neurons of the primary auditory cortex in the *Fmr1* KO mice showed a significant increase of dendritic spine density on apical tufts (WT 0.71±0.09 spines/µm, KO 1.11±0.19 spines/µm; $p<0.05$) that was not observed in the basal dendrites (WT 0.58±0.10 spines/µm, KO 0.58±0.08 spines/µm; $p=0.98$) (**Figure 4b**). Hence, the auditory cortex of KO mice exhibit a similar phenotype as the barrel cortex in regards to the spine densities on apical and basal dendrites of layer 5 pyramidal neurons.

Examination next shifted to the visual region of the sensory cortex, which is responsible for the processing of visual stimuli. Although mice do not have a highly refined sense of vision compared to higher order mammals such as primates, and the percentage of cortex devoted to visual processing is considerably smaller, this remains an important area for investigation nonetheless as patients with FXS display

a propensity for vision and eye disorders such as strabismus, ptosis, and nystagmus (Hersh and Saul, 2011).

In the visual cortex, the result of *Fmr1* silencing on the alteration in L5 neuron dendritic spine densities in *Fmr1* KO mice is similar to what was observed in the other sensory cortices. Apical tufts of layer 5 neurons of adult KO animals displayed increased spine density (WT 0.74±0.12 spines/µm, KO 1.19±0.07 spines/µm; $p<0.01$) while the basal dendrites of the same cells showed no significant difference (WT 0.57±0.07 spines/µm, KO 0.56±0.06 spines/µm; $p=0.75$) (**Figure 5b**).

These data show that loss of FMRP expression indeed affects the density of dendritic spines of layer 5 pyramidal neurons consistently across sensory cortices in adult animals. More specifically, this loss specifically affects the apical tufts of these neurons while the basal dendrites are unaffected. This consistent effect is observed in multiple sensory cortices and suggests that sensory processing may be altered across several modalities. The fact that this affect is seen across multiple sensory areas in the *Fmr1* KO animals suggests that this may contribute or be the cause of an altered processing of sensory input in FXS.

3.4 Dendritic spine density is altered in adult but not adolescent *Fmr1* KO mice

During the course of normal development, the density of cortical dendritic spines peaks prior to adolescence and gradually decreases over adolescence as the neural circuitry is fine tuned and remodeled (Hara et al., 2011; Purves and Lichtman, 1980). To investigate the time frame of the abnormality of dendritic spine density in

KO mice, quantification of the density of dendritic protrusions in one month old adolescent mice and four month old adult mice was performed. Using bright field immunohistochemistry, tracings of dendritic structures and spines were done to determine whether there are differences in density profiles between apical and basal dendrites of barrel cortex neurons in WT and KO mice at different ages.

On the apical tufts of barrel field pyramidal layer 5 neurons of one month old animals both WT and KO mice exhibited similar spine densities (WT 1.22±0.14 spines/µm, KO 1.30±0.05 spines/µm; p=0.3) (**Figure 2d**). This result is in contrast to the significant differences in apical dendrite spine densities of adult WT and KO animals. Similar to adult animals, the basal dendrites of L5 neurons were not significantly different between WT and KO animals at one month of age (WT 0.55±0.07 spines/µm, KO 0.54±0.06 spines/µm; p=0.97). This shows that the increased density of dendritic spines is present in adult KO animals, but is absent at one month of age. The fact that the increased spine density on apical dendrites only appears in adulthood and not during adolescence, suggests that the lack of FMRP in these neurons may disrupt the normal developmental spine pruning mechanisms that normally occur in the cortex.

Next was asked whether the relationship between spine density and branch order observed in the adult cohort is also present during adolescence. Indeed, it was found that apical dendrites show a significant decrease in spine density as branch order increases, and this was maintained in both WT and KO animals at this age (two-

way ANOVA: $F(5, 100)=76.47$, $p<0.001$) (**Figure 3b**). spine density also changed significantly with branch order in the basal dendrites, however, in contrast to the apical dendrites, spine density increased with branch order (two-way ANOVA: $F(3, 54)=7.14$, $p<0.001$). Similar to the adult animals, the trend of spine density across branch orders was very consistent. Although there was an observed difference of spine density when comparing different branch orders, when considering branch order along with genotype, there is no significant difference in either apical or basal dendrites (unlike the apical dendrites of adult mice) (**Figure 3b**). This indicates that the average spine density of any specific branch order is similar across genotypes.

3.5 Layer II/III pyramidal cells of *Fmr1* KO mice do not display increased spine density

To determine if the increase in spine density of apical dendrites in *Fmr1* KO mice is specific to pyramidal neurons of layer 5, analysis was repeated in the pyramidal cells of cortical layer 2/3. Layer 2/3 of the cerebral cortex is the primary target for interhemispheric corticocortical afferents and is the principal source of efferents to other cortical regions. This region is a very important area for communication of neurons within the cortex and as such, warrants investigation in *Fmr1* KO mice. Although the majority of GFP expressing cortical cells in the GFP-M line of mice are found in layer 5, cells of layer 2/3 will also express GFP after the animal has entered adulthood (**Figure 6a**). This allowed examination of layer 2/3 pyramidal neurons in the barrel field of the somatosensory cortex in adult animals to

investigate if the spine phenotype previously detected in layer 5 neurons of KO mice could also be observed in the neurons of this layer. In contrast to the abnormal phenotype that was observed in the apical dendrites of layer 5 neurons, no significant difference in dendritic spine density was observed in either apical (WT 1.21±0.17 spines/µm, KO 1.31±0.08 spines/µm; p=0.32) or basal segments (WT 1.23±0.16 spines/µm, KO 1.21±0.19 spines/µm; p=0.89) (**Figure 6d**). This suggests that the spine density phenotype of KO animals may be specific to L5 neurons.

3.6 Spine density is increased in both apical and basal dendrites of CA1 hippocampal neurons in *Fmr1* KO mice

In addition to the cortex, the hippocampus is also plays a critical role in proper cognitive function. The hippocampus is part of the limbic system and plays a key role in the consolidation of information, short-term as well as long-term memory, and spatial learning and awareness (Deiana et al., 2011; Opitz, 2014; Retailleau et al., 2012). Animals (as well as human patients) suffering from FXS have cognitive impairments, which include learning and memory deficits, and tend to perform poorly at varying spatial awareness tasks such as the Morris water maze and trace fear memory tests (Frank Kooy, 2003; Godfraind et al., 1996; Neuwirth et al., 2015). Therefore, it was next asked if hippocampal neurons of the *Fmr1* KO mice showed any abnormalities of dendritic spine density in either apical or basal compartments similar to layer 5 pyramidal cells of the cortex.

Hippocampal cells of the GFP-M line mice exhibit excellent labeling which allows the tracing of these cells in both the WT and *Fmr1* KO mice (**Figure 7a,b**). The structure of the hippocampus is generally separated into different regions. The CA1 region contains many pyramidal neurons and is the first region in the hippocampal circuit that yields a significant output pathway leading to the entorhinal cortex and subiculum. Being the primary source of output from the hippocampus, the cells of this region were targeted for investigation.

It was found that the *Fmr1* KO mice showed increased dendritic spine density in both apical (WT 1.12±0.04 spines/µm, KO 1.52±0.19 spines/µm; $p<0.05$) and basal compartments (WT 1.01±0.05 spines/µm; KO 1.25±0.10 spines/µm; $p<0.05$) compared to WT animals (**Figure 8b**). This finding in hippocampal neurons differs from the findings in cortical neurons in that the spine density increase in CA1 pyramidal neurons is not specific to the apical segments but is increased in both dendritic compartments of these neurons.

3.7 Heterozygous females display spine density similar to KOs in L5 neurons of sensory cortices

Up until this point, this investigation has focused on comparing *Fmr1* KO animals with WTs. Now the question shifts to how females, which carry two copies of the X chromosome, may be affected when their genome consists of one WT copy of the allele and one mutant allele. It is possible that these individuals may display a phenotype fully resembling that of WT or of KO animals. They may also consist of

two distinct populations of cells, one resembling that of the KOs and one resembling WT. Yet another possibility is that this HET group may display an altogether unique phenotype laying somewhere on a spectrum between the two other genotypes. These female HET mice were next to be analyzed to investigate whether spine density is altered in these animals.

Using fluorescent immunohistochemistry, the pattern of expression of FMRP was examined in HET animals, and (as was done previously) the percentage of GFP expressing cells that also express FMRP were quantified. In HET females, there was an approximately 50% chance that any GFP positive cell also showed FMRP labeling (55.6±3.9%) (**Figure 1b**). There was no discernible pattern to the distribution of FMRP positive neurons in the cortex, and by eye, the intensity of the FMRP label was consistent with that observed in the WT animals. This result is consistent with the random X chromosome inactivation which occurs in the cells of females, and may lead to a mosaic pattern of FMRP expression.

Dendritic tracings of layer 5 neurons were then performed in different cortical regions as well as hippocampal CA1 cells in adult HET females. Layer 2/3 neurons were not included in this analysis as the KO animals displayed no abnormal phenotype when compared to WTs. In layer 5 pyramidal cells of the barrel cortex, dendritic spine density in HET mice was significantly increased compared to WTs on the apical tufts (WT 0.6±0.05 spines/µm, HET 0.87±0.11 spines/µm; $p<0.005$), while the basal dendrites showed no significant difference in spine density (WT 0.55±0.07

spines/µm, HET 0.56±0.07 spines/µm; p=0.73). This effect closely resembled what was observed in the *Fmr1* KO animals (**Figure 2d**) and the HETs showed no significant difference when compared to KOs (p>0.05) and seem to very closely resemble these animals in regards to the spine density phenotype. This effect in HET mice was observed not only in the barrel cortex, but also in the auditory (Apical: 1.02±0.19 spines/µm. Basal: 0.67±0.09 spines/µm) (**Figure 4b**) and visual cortices (Apical: 1.15±0.16 spines/µm. Basal: 0.56±0.08 spines/µm) as well (**Figure 5b**).

3.8 Heterozygous females display spine density similar to WTs in CA1 neurons of hippocampus

In the CA1 neurons of the hippocampus, investigation was done on how spine density in HET animals compares to that of WT and *Fmr1* KOs. In adult HET females, the CA1 neurons spine density is similar to the WT animals in regards to dendritic spine density (Apical: 1.23±0.11 spines/µm. Basal: 1.22±0.18 spines/µm) (**Figure 8b**). The apical dendrites of the HETs are not significantly different compared to the WTs, but do show a significantly lower spine density than the KOs (p<0.05). There were no significant differences seen on basal dendrites of HET animals compared to either KO (p=0.77) or WT (p=0.07) animals. These findings suggest that spine densities of CA1 hippocampal neurons in HET mice seem to more closely resemble the dendritic spine density seen in WTs (although the result is not significant).

Chapter 4: DISCUSSION

Individuals suffering from FXS obtain little to no relief from the treatments currently available and much remains unknown regarding the neurobiology underlying this disorder, despite the long history of investigation in the field. The increased density of dendritic spines has long been seen in both human autopsy tissue as well as the mouse model of the disorder, and is widely viewed as a hallmark of FXS (Bassell and Warren, 2008; Comery et al., 1997; Garber et al., 2008; Irwin et al., 2001; McLennan et al., 2011; Nimchinsky et al., 2001). In spite of this, many have overlooked, or failed to notice, the potentially unequal affect that may be present in differing neuron types as well as on differing dendritic compartments of the same cell. A survey of other studies that have looked at spine densities of different cell types in FXS tend to report conflicting results, some of which report increased spine density and others that report densities similar to WT (Comery et al., 1997; Hayashi et al., 2007; Irwin et al., 2001; Nimchinsky et al., 2001; Portera-Cailliau, 2012). All of the fixed tissue studies to this point have been done using Golgi staining, while the method employed in the present study breaks from this convention. This investigation, using a transgenic mouse line and immunohistochemisty to label cells for fixed tissue imaging, is the first of its kind and has resulted in findings previously unseen, or perhaps overlooked, in the investigation of FXS.

In this study, visualization of the expression pattern of FMRP in the three genotypes was performed first. As expected, nearly all of GFP-expressing cells in

WT GFPM line mice exhibited expression of FMRP, while nearly all of GFP-expressing cells in the KOs did not (**Figure 1b**). The HET mice displayed a mosaic pattern with approximately 50% of GFP-expressing cells also expressing FMRP. These findings validated the *Fmr1* KO mouse model for further investigation of the dendritic spine phenotype in FXS. Using the GFPM transgenic mouse line and immunohistochemistry, dendritic spine density was quantified in different neurons, cortical regions, and dendritic compartments in the three genotypes.

When comparing the WT and KO animals, it was found that dendritic spine density was significantly increased in the apical dendrites of the *Fmr1* KOs while the basal dendrites were unaffected in all layer 5 neurons across multiple cortical regions (**Figure 2d, 4b, 5b**). In contrast, increased spine density was not observed on either apical or basal dendrites of layer 2/3 neurons (**Figure 6d**). Furthermore, spine density alterations were specific to adult KOs and not observed in adolescent animals (**Figure 2d**). In addition, it was also found that adult hippocampal neurons display an increase of dendritic spines in both apical as well as basal dendrites in *Fmr1* KO mice (**Figure 8b**).

The finding that different dendritic compartments of layer 5 pyramidal cells are not affected equally by the lack of FMRP is novel and interesting. This finding suggests that the increase of dendritic spine density characteristically seen in FXS is unique to specific dendritic compartments of layer 5 pyramidal cells. While the superficial regions of the apical dendrites show a robust increase in dendritic spines,

the basal dendrites are spared from this abnormality. As a result of this, it is not unreasonable to imagine that the defect seen in FXS may be due to a specific circuitry and connectivity defect rather than a global irregularity that is characteristic of an entire cell. This may, in fact, be the case since connections from specific brain areas have been found to synapse preferentially on specific parts of dendrites of a neuron (Rah et al., 2013; Schoonover et al., 2014).

Synapses on apical and basal dendritic branches are likely participants of differing neuronal circuitry. In fact, a recent study investigating thalamocortical synapses on layer 5 neurons found that the vast majority of these connections are made on basal dendrites (Rah et al., 2013). Apical dendrites did contain some connections from the thalamus, but these were few and found only in the proximal apical shaft close to the soma. The apical tufts, the primary region in which a significant difference in spine density between genotypes was found in this study, are known to have very few thalamocortical connections (Rah et al., 2013). In light of this, it is not unreasonable to imagine that the loss of FMRP expression may not influence thalamocortical synapses very strongly. Since the motor thalamus is known to be responsible for gross general movement and locomotion (Grillner and Wallén, 2004; Baker, 2011; Kawai et al., 2015), and motor cortex is responsible for fine skilled movements (Hosp et al., 2013; Kawai et al., 2015), this could explain the skilled motor learning defect seen in FXS. General locomotion of *Fmr1* KO mice does not seem to be affected, but KO animals display a significant inability to learn a skilled motor task (Padmashri et al., 2013; Santos et al., 2014).

Assuming that these thalamocortical synapses are unaltered in the KOs, further investigation of if and how exactly these synapses differ from others (corticocortical connections for example) may help shed light on the specific role FMRP plays locally at the synapse. It is also possible that a certain type of synaptic connections is affected by FMRP loss, and all other types (including thalamocortical synapses) are unaffected. Investigation and categorization of synapses at the molecular level will be necessary to advance the understanding of synapse disruption in FXS. The synapses found at the apical tufts of layer 5 neurons may be of a very specific type and may show unique molecular signatures and expression patterns of different proteins such as PSD95, synaptopodin, VGluT1/2, etc. Furthermore, spines of varying morphologies could conceivably exhibit similarly unique expression patterns of various proteins. Numerous investigations of FXS have reported an abundance of long, thin dendritic spines (Comery et al., 1997; Irwin et al., 2001), and it is possible that these spines not only show this characteristic morphology, but a characteristic molecular signature as well. The future study of how synapses may differ at the molecular level will be very telling and yield insight into FXS among a multitude of other topics as well.

Chapter 5: CONCLUSION

FXS is prevalent in the general population and many individuals struggle with the disorder with very little aid from the current forms of therapy and pharmaceuticals available. Living with an intellectual disability can be extremely challenging not only for the person affected but also for their families who take on the burden of care. Individuals suffering from FXS deserve a life of meaning, and aiding them with effective drugs and therapies will not only serve these individuals and their families, but also society as a whole by allowing them to make meaningful contributions the their communities.

The work done on this project, and the resulting knowledge gleaned, will surely help advance our understanding of FXS. Studies of the effect that *FMR1* silencing has at the cellular and synapse level has previously failed to observe the specific synaptic findings I have shown here. With this increased level of understanding comes new and more accurate ways of thinking about FXS and could open new doors to possible treatments. It is my hope that this work will make a substantial impact in the field and enable investigators to rethink and reassess their theories of FXS. One day this knowledge, along with other breakthroughs in the field of FXS, will lead to a substantial increase in the efficacy of treatments and quality of life of those who suffer from this disorder.

References

Ashley, C.T., Sutcliffe, J.S., Kunst, C.B., Leiner, H.A., Eichler, E.E., Nelson, D.L., and Warren, S.T. (1993). Human and murine FMR-1: alternative splicing and translational initiation downstream of the CGG–repeat. Nat. Genet. *4*, 244–251.

Baker, S.N. (2011). The primate reticulospinal tract, hand function and functional recovery. J. Physiol. *589*, 5603–5612.

Bassell, G.J., and Warren, S.T. (2008). Fragile X Syndrome: Loss of Local mRNA Regulation Alters Synaptic Development and Function. Neuron *60*, 201–214.

Bear, M.F., Huber, K.M., and Warren, S.T. (2004). The mGluR theory of fragile X mental retardation. Trends Neurosci. *27*, 370–377.

Bellot, A., Guivernau, B., Tajes, M., Bosch-Morató, M., Valls-Comamala, V., and Muñoz, F.J. (2014). The structure and function of actin cytoskeleton in mature glutamatergic dendritic spines. Brain Res. *1573*, 1–16.

Brouwer, J., Mientjes, E., Bakker, C., Nieuwenhuizen, I., Severijnen, L., Van der Linde, H., Nelson, D., Oostra, B., and Willemsen, R. (2007). Elevated Fmr1 mRNA levels and reduced protein expression in a mouse model with an unmethylated Fragile X full mutation. Exp. Cell Res. *313*, 244–253.

Brown, V., Jin, P., Ceman, S., Darnell, J.C., O'Donnell, W.T., Tenenbaum, S.A., Jin, X., Feng, Y., Wilkinson, K.D., Keene, J.D., et al. (2001). Microarray Identification of FMRP-Associated Brain mRNAs and Altered mRNA Translational Profiles in Fragile X Syndrome. Cell *107*, 477–487.

Chen, E., and Joseph, S. (2015). Fragile X mental retardation protein: A paradigm for translational control by RNA-binding proteins. Biochimie *114*, 147–154.

Cheng, M.K., and Disteche, C.M. (2004). Silence of the fathers: Early X inactivation. BioEssays *26*, 821–824.

Cochran, D.M., Sikoglu, E.M., Hodge, S.M., Edden, R.A.E., Foley, A., Kennedy, D.N., Moore, C.M., and Frazier, J.A. (2015). Relationship Among Glutamine, γ-Aminobutyric Acid, and Social Cognition In Autism Spectrum Disorders. J. Child Adolesc. Psychopharmacol.

Coffee, B., Keith, K., Albizua, I., Malone, T., Mowrey, J., Sherman, S.L., and Warren, S.T. (2009). Incidence of Fragile X Syndrome by Newborn Screening for Methylated FMR1 DNA. Am. J. Hum. Genet. *85*, 503–514.

Comery, T.A., Harris, J.B., Willems, P.J., Oostra, B.A., Irwin, S.A., Weiler, I.J., and Greenough, W.T. (1997). Abnormal dendritic spines in fragile X knockout mice: Maturation and pruning deficits. Proc. Natl. Acad. Sci. U. S. A. *94*, 5401–5404.

Consorthium, T.D.-B.F.X., Bakker, C.E., Verheij, C., Willemsen, R., van der Helm, R., Oerlemans, F., Vermey, M., Bygrave, A., Hoogeveen, A., Oostra, B.A., et al. (1994). Fmr1 knockout mice: A model to study fragile X mental retardation. Cell *78*, 23–33.

Cruz-Martín, A., Crespo, M., and Portera-Cailliau, C. (2010). Delayed Stabilization of Dendritic Spines in Fragile X Mice. J. Neurosci. *30*, 7793–7803.

Dansie, L.E., Phommahaxay, K., Okusanya, A.G., Uwadia, J., Huang, M., Rotschafer, S.E., Razak, K.A., Ethell, D.W., and Ethell, I.M. (2013). Long-lasting effects of minocycline on behavior in young but not adult Fragile X mice. Neuroscience *246*, 186–198.

Darnell, J.C., Van Driesche, S.J., Zhang, C., Hung, K.Y.S., Mele, A., Fraser, C.E., Stone, E.F., Chen, C., Fak, J.J., Chi, S.W., et al. (2011). FMRP Stalls Ribosomal Translocation on mRNAs Linked to Synaptic Function and Autism. Cell *146*, 247–261.

Deiana, S., Platt, B., and Riedel, G. (2011). The cholinergic system and spatial learning. Behav. Brain Res. *221*, 389–411.

Feng, G., Mellor, R.H., Bernstein, M., Keller-Peck, C., Nguyen, Q.T., Wallace, M., Nerbonne, J.M., Lichtman, J.W., and Sanes, J.R. (2000). Imaging Neuronal Subsets in Transgenic Mice Expressing Multiple Spectral Variants of GFP. Neuron *28*, 41–51.

Frank Kooy, R. (2003). Of mice and the fragile X syndrome. Trends Genet. *19*, 148–154.

Galvez, R., and Greenough, W.T. (2005). Sequence of abnormal dendritic spine development in primary somatosensory cortex of a mouse model of the fragile X mental retardation syndrome. Am. J. Med. Genet. A. *135A*, 155–160.

Garber, K.B., Visootsak, J., and Warren, S.T. (2008). Fragile X syndrome. Eur. J. Hum. Genet. EJHG *16*, 666–672.

Godfraind, J.M., Reyniers, E., De Boulle, K., D'Hooge, R., De Deyn, P.P., Bakker, C.E., Oostra, B.A., Kooy, R.F., and Willems, P.J. (1996). Long-term potentiation in the hippocampus of fragile X knockout mice. Am. J. Med. Genet. *64*, 246–251.

Grillner, S., and Wallén, P. (2004). Innate versus learned movements - A false dichotomy?

Hagerman, P.J. (2008). The fragile X prevalence paradox. J. Med. Genet. *45*, 498–499.

Hagerman, R., Hoem, G., and Hagerman, P. (2010). Fragile X and autism: Intertwined at the molecular level leading to targeted treatments. Mol. Autism *1*, 12.

Hall, S.S., Burns, D.D., Lightbody, A.A., and Reiss, A.L. (2008). Longitudinal Changes in Intellectual Development in Children with Fragile X Syndrome. J. Abnorm. Child Psychol. *36*, 927–939.

Hara, Y., Rapp, P.R., and Morrison, J.H. (2011). Neuronal and morphological bases of cognitive decline in aged rhesus monkeys. AGE *34*, 1051–1073.

Hayashi, M.L., Rao, B.S.S., Seo, J.-S., Choi, H.-S., Dolan, B.M., Choi, S.-Y., Chattarji, S., and Tonegawa, S. (2007). Inhibition of p21-activated kinase rescues symptoms of fragile X syndrome in mice. Proc. Natl. Acad. Sci. U. S. A. *104*, 11489–11494.

Hersh, J.H., and Saul, R.A. (2011). Health Supervision for Children With Fragile X Syndrome. Pediatrics *127*, 994–1006.

Hosp, J.A., Mann, S., Wegenast-Braun, B.M., Calhoun, M.E., and Luft, A.R. (2013). Region and task-specific activation of Arc in primary motor cortex of rats following motor skill learning. Neuroscience *250*, 557–564.

Iliff, A.J., Renoux, A.J., Krans, A., Usdin, K., Sutton, M.A., and Todd, P.K. (2013). Impaired activity-dependent FMRP translation and enhanced mGluR-dependent LTD in Fragile X premutation mice. Hum. Mol. Genet. *22*, 1180–1192.

Irwin, S.A., Patel, B., Idupulapati, M., Harris, J.B., Crisostomo, R.A., Larsen, B.P., Kooy, F., Willems, P.J., Cras, P., Kozlowski, P.B., et al. (2001). Abnormal dendritic spine characteristics in the temporal and visual cortices of patients with fragile-X syndrome: A quantitative examination. Am. J. Med. Genet. *98*, 161–167.

Isshiki, M., Tanaka, S., Kuriu, T., Tabuchi, K., Takumi, T., and Okabe, S. (2014). Enhanced synapse remodelling as a common phenotype in mouse models of autism. Nat. Commun. *5*.

Kaibara, T., and Leung, L.S. (1993). Basal versus apical dendritic long-term potentiation of commissural afferents to hippocampal CA1: a current-source density study. J. Neurosci. *13*, 2391–2404.

Kawai, R., Markman, T., Poddar, R., Ko, R., Fantana, A.L., Dhawale, A.K., Kampff, A.R., and Ölveczky, B.P. (2015). Motor Cortex Is Required for Learning but Not for Executing a Motor Skill. Neuron *86*, 800–812.

Klein, M.E., Castillo, P.E., and Jordan, B.A. (2015). Coordination between Translation and Degradation Regulates Inducibility of mGluR-LTD. Cell Rep. *10*, 1459–1466.

Lefebvre, J.L., Sanes, J.R., and Kay, J.N. (2015). Development of Dendritic Form and Function. Annu. Rev. Cell Dev. Biol. *31*, null.

McLennan, Y., Polussa, J., Tassone, F., and Hagerman, R. (2011). Fragile X Syndrome. Curr. Genomics *12*, 216–224.

Muhammad, A., Carroll, C., and Kolb, B. (2012). Stress during development alters dendritic morphology in the nucleus accumbens and prefrontal cortex. Neuroscience *216*, 103–109.

Mychasiuk, R., Muhammad, A., Gibb, R., and Kolb, B. (2013). Long-term alterations to dendritic morphology and spine density associated with prenatal exposure to nicotine. Brain Res. *1499*, 53–60.

Neuwirth, L.S., Volpe, N.P., Ng, S., Marsillo, A., Corwin, C., Madan, N., Ferraro, A.M., and El Idrissi, A. (2015). Taurine recovers mice emotional learning and memory disruptions associated with fragile x syndrome in context fear and auditory cued-conditioning. Adv. Exp. Med. Biol. *803*, 425–438.

Nimchinsky, E.A., Oberlander, A.M., and Svoboda, K. (2001). Abnormal Development of Dendritic Spines inFMR1 Knock-Out Mice. J. Neurosci. *21*, 5139–5146.

Opitz, B. (2014). Memory function and the hippocampus. Front. Neurol. Neurosci. *34*, 51–59.

Padmashri, R., Reiner, B.C., Suresh, A., Spartz, E., and Dunaevsky, A. (2013). Altered Structural and Functional Synaptic Plasticity with Motor Skill Learning in a Mouse Model of Fragile X Syndrome. J. Neurosci. *33*, 19715–19723.

Portera-Cailliau, C. (2012). Which Comes First in Fragile X Syndrome, Dendritic Spine Dysgenesis or Defects in Circuit Plasticity? The Neuroscientist *18*, 28–44.

Purves, D., and Lichtman, J.W. (1980). Elimination of Synapses in the Developing Nervous System. Science *210*, 153–157.

Rah, J.-C., Bas, E., Colonell, J., Mishchenko, Y., Karsh, B., Fetter, R.D., Myers, E.W., Chklovskii, D.B., Svoboda, K., Harris, T.D., et al. (2013). Thalamocortical input onto layer 5 pyramidal neurons measured using quantitative large-scale array tomography. Front. Neural Circuits *7*.

Retailleau, A., Etienne, S., Guthrie, M., and Boraud, T. (2012). Where is my reward and how do I get it? Interaction between the hippocampus and the basal ganglia during spatial learning. J. Physiol.-Paris *106*, 72–80.

Risher, W.C., Patel, S., Kim, I.H., Uezu, A., Bhagat, S., Wilton, D.K., Pilaz, L.-J., Singh Alvarado, J., Calhan, O.Y., Silver, D.L., et al. Astrocytes refine cortical connectivity at dendritic spines. eLife *3*.

Rotschafer, S.E., and Razak, K.A. (2014). Auditory Processing in Fragile X Syndrome. Front. Cell. Neurosci. *8*.

Rotschafer, S., and Razak, K. (2013). Altered auditory processing in a mouse model of fragile X syndrome. Brain Res. *1506*, 12–24.

Santoro, M.R., Bray, S.M., and Warren, S.T. (2012). Molecular Mechanisms of Fragile X Syndrome: A Twenty-Year Perspective. Annu. Rev. Pathol. Mech. Dis. *7*, 219–245.

Santos, A.R., Kanellopoulos, A.K., and Bagni, C. (2014). Learning and behavioral deficits associated with the absence of the fragile X mental retardation protein: what a fly and mouse model can teach us. Learn. Mem. *21*, 543–555.

Schoonover, C.E., Tapia, J.-C., Schilling, V.C., Wimmer, V., Blazeski, R., Zhang, W., Mason, C.A., and Bruno, R.M. (2014). Comparative Strength and Dendritic Organization of Thalamocortical and Corticocortical Synapses onto Excitatory Layer 4 Neurons. J. Neurosci. *34*, 6746–6758.

Steele, J.W., Brautigam, H., Short, J.A., Sowa, A., Shi, M., Yadav, A., Weaver, C.M., Westaway, D., Fraser, P.E., St George-Hyslop, P.H., et al. (2014). Early fear memory defects are associated with altered synaptic plasticity and molecular architecture in the TgCRND8 Alzheimer's disease mouse model. J. Comp. Neurol. *522*, 2319–2335.

Tranfaglia, M.R. (2011). The Psychiatric Presentation of Fragile X: Evolution of the Diagnosis and Treatment of the Psychiatric Comorbidities of Fragile X Syndrome. Dev. Neurosci. *33*, 337–348.

Verkerk, A.J.M.H., Pieretti, M., Sutcliffe, J.S., Fu, Y.-H., Kuhl, D.P.A., Pizzuti, A., Reiner, O., Richards, S., Victoria, M.F., Zhang, F., et al. (1991). Identification of a gene (FMR-1) containing a CGG repeat coincident with a breakpoint cluster region exhibiting length variation in fragile X syndrome. Cell *65*, 905–914.

Yuskaitis, C.J., Beurel, E., and Jope, R.S. (2010). Evidence of reactive astrocytes but not peripheral immune system activation in a mouse model of Fragile X Syndrome. Biochim. Biophys. Acta *1802*, 1006–1012.

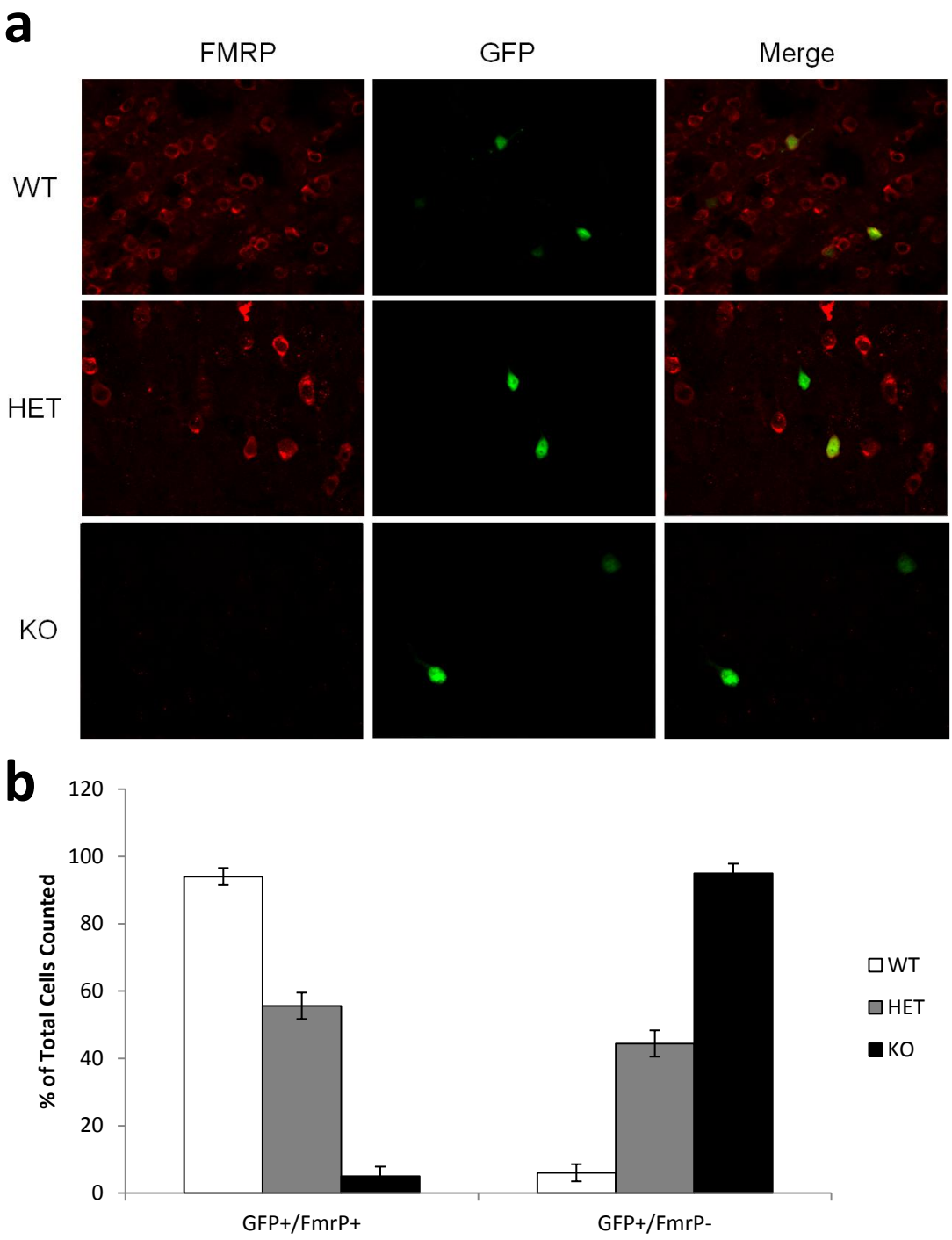

Figure 1. a, Immunofluorescent images of cortical coronal sections showing FMRP labeling (red) and endogenous GFP-expressing layer 5 pyramidal neurons (green) in barrel cortex of one-month old *Fmr1* KO, heterozygous, and wild-type mice. **b,** Percentages of GFP-expressing cortical neurons with or without FMRP labeling in different groups (mean±s.d.).

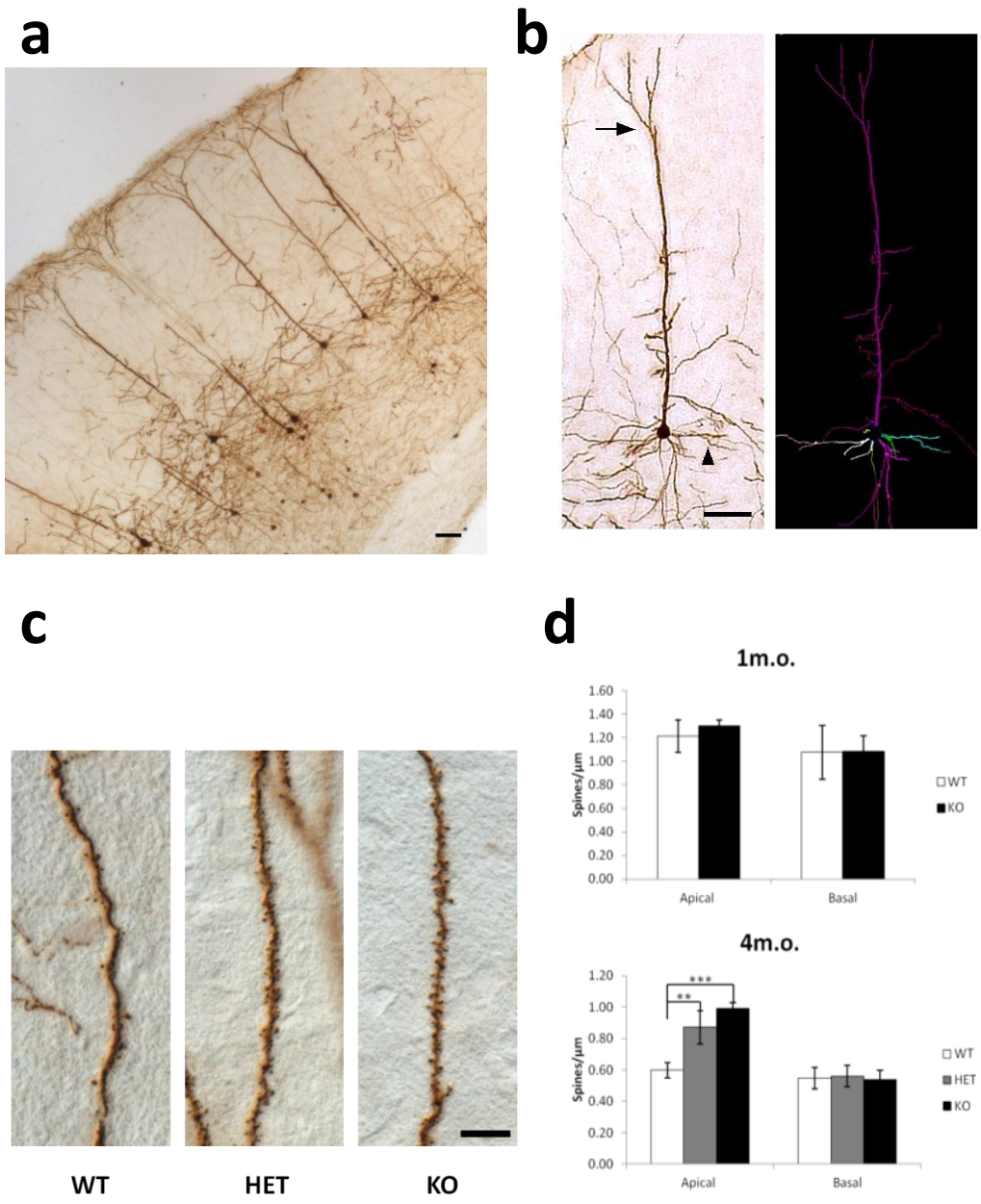

Figure 2. a, GFP immunolabeled layer 5 pyramidal cells. **b,** Layer 5 neuron of the barrel cortex (left) and its tracing (right). Arrow indicates apical segment, arrowhead indicates basal segment. **c,** Immunolabeled apical segments of layer 5 neurons of barrel cortex. **d,** Average spine densities on apical and basal dendrites of barrel cortex layer 5 pyramidal cells in WT, HET and *Fmr1* KO mice at 1 and 4 months of age (mean±s.d.). **indicates p<0.01; ***indicates p<0.001. Scale Bars: 50µm (a), 50µm (b), 25µm (c).

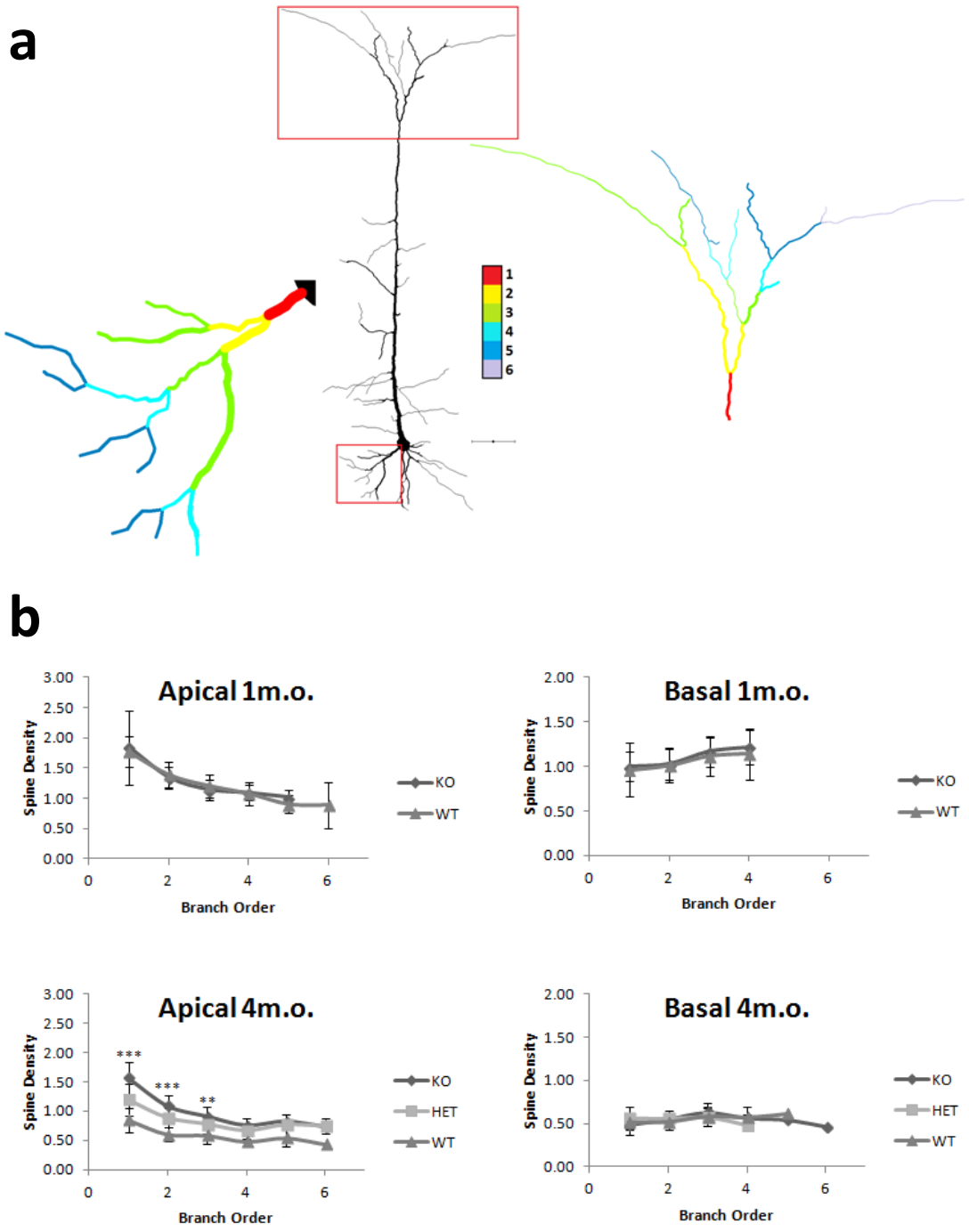

Figure 3. a, Tracing of a barrel cortex layer 5 pyramidal cell with color coding to indicate branch order along apical and basal dendrites. Scale bar: 50µm **b,** Average spine densities (spines per µm) by branch order for both apical and basal dendrites of layer 5 pyramidal cells of barrel cortex in 1 and 4 month old mice (mean±s.d.). ***indicates p<0.001; **indicates p<0.01.

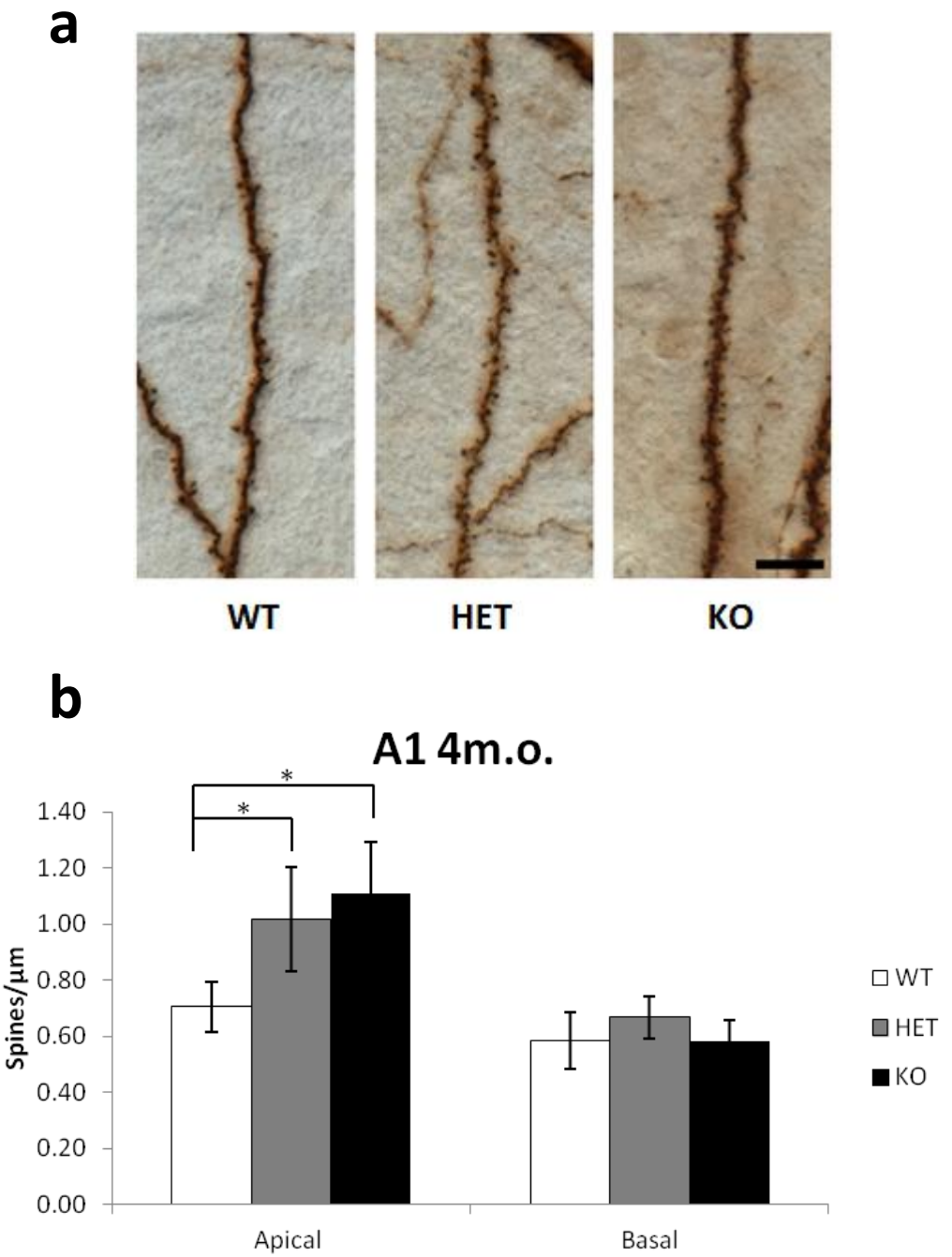

Figure 4. a, Immunolabeled apical segments of layer 5 neurons of primary auditory cortex. Scale bar: 25µm **b,** Average spine density of apical and basal dendrites of primary auditory cortex layer 5 pyramidal neurons in 4 month old mice (mean±s.d.). *indicates $p<0.05$.

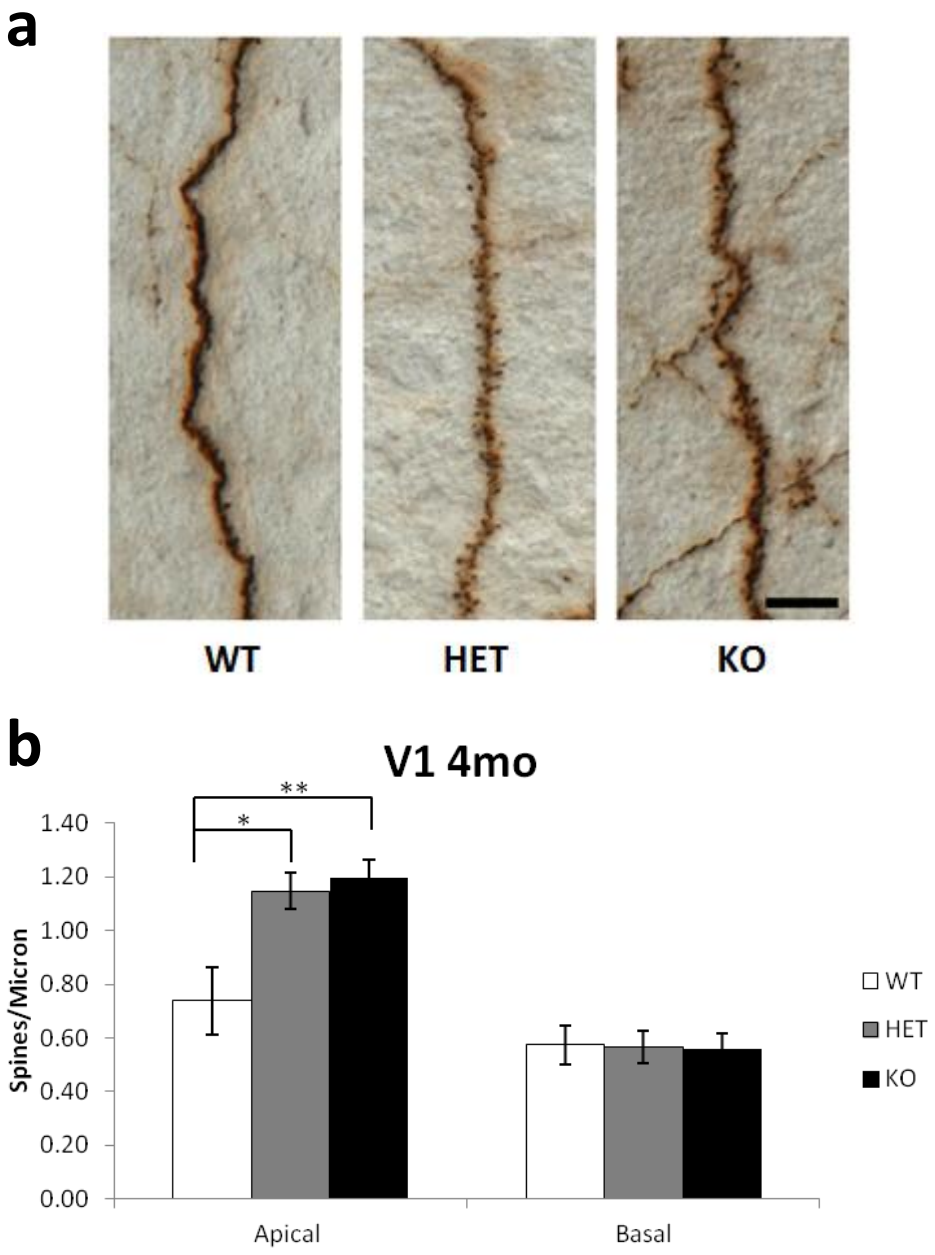

Figure 5. a, Immunolabeled apical segments of primary visual cortex layer 5 neurons. Scale bar: 25µm **b,** Average spine density of apical and basal dendrites of primary visual cortex layer 5 pyramidal cells in 4 month old mice (mean±s.d.). *indicates $p<0.05$; **indicates $p<0.01$.

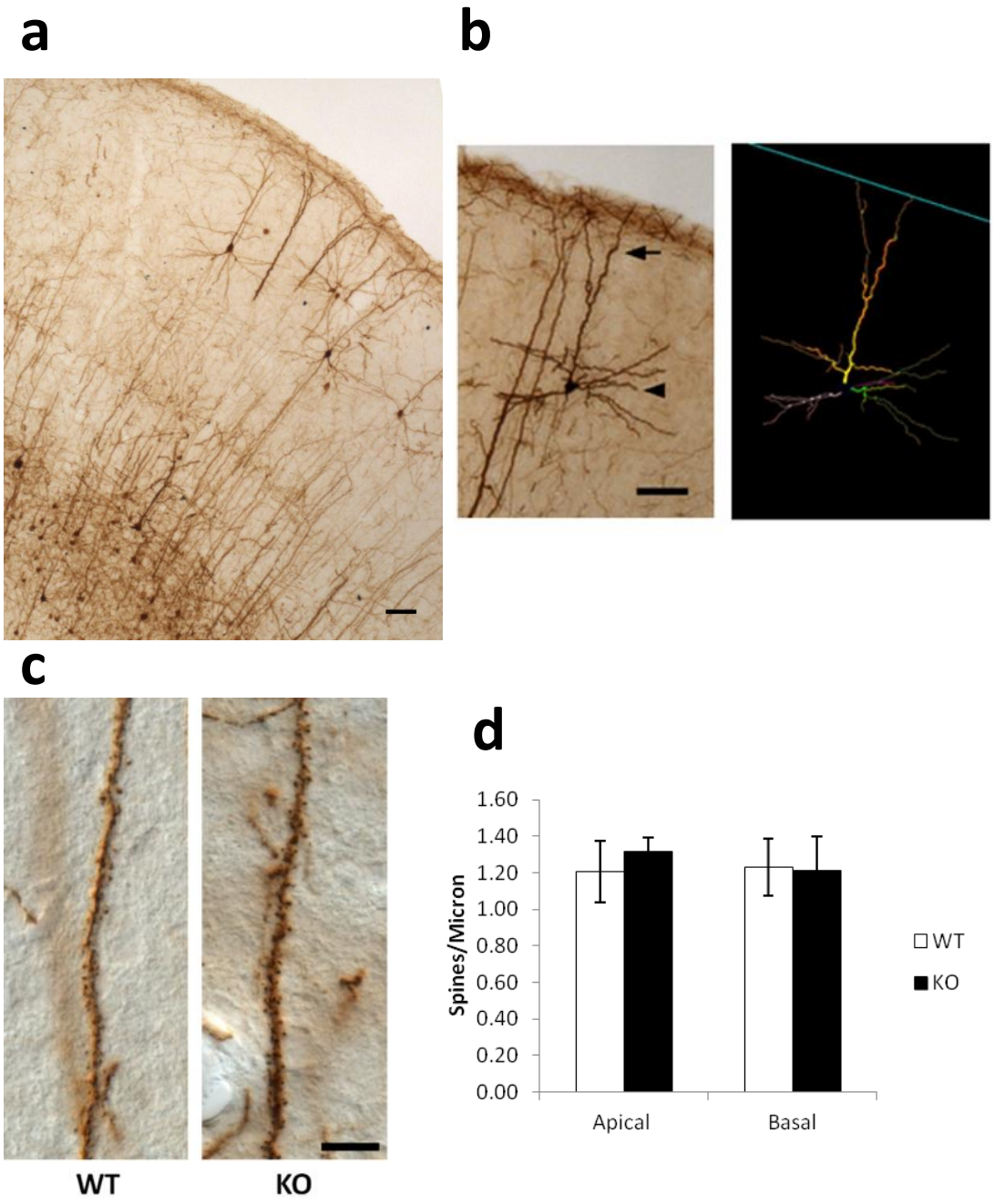

Figure 6. a, GFP immunolabeled layer 2/3 pyramidal cells. **b,** Layer 2/3 neuron of the barrel cortex and its tracing. Arrow indicates apical segment, arrowhead indicates basal segment. **c,** Immunolabeled apical segments of layer 2/3 neurons of barrel cortex. **d,** Average spine densities in apical and basal dendrites of WT and *Fmr1* KO mice in layer 2/3 pyramidal cells of barrel cortex of 4 month old mice (mean±s.d.). Scale Bars: 50µm (a), 50µm (b), 25µm (c).

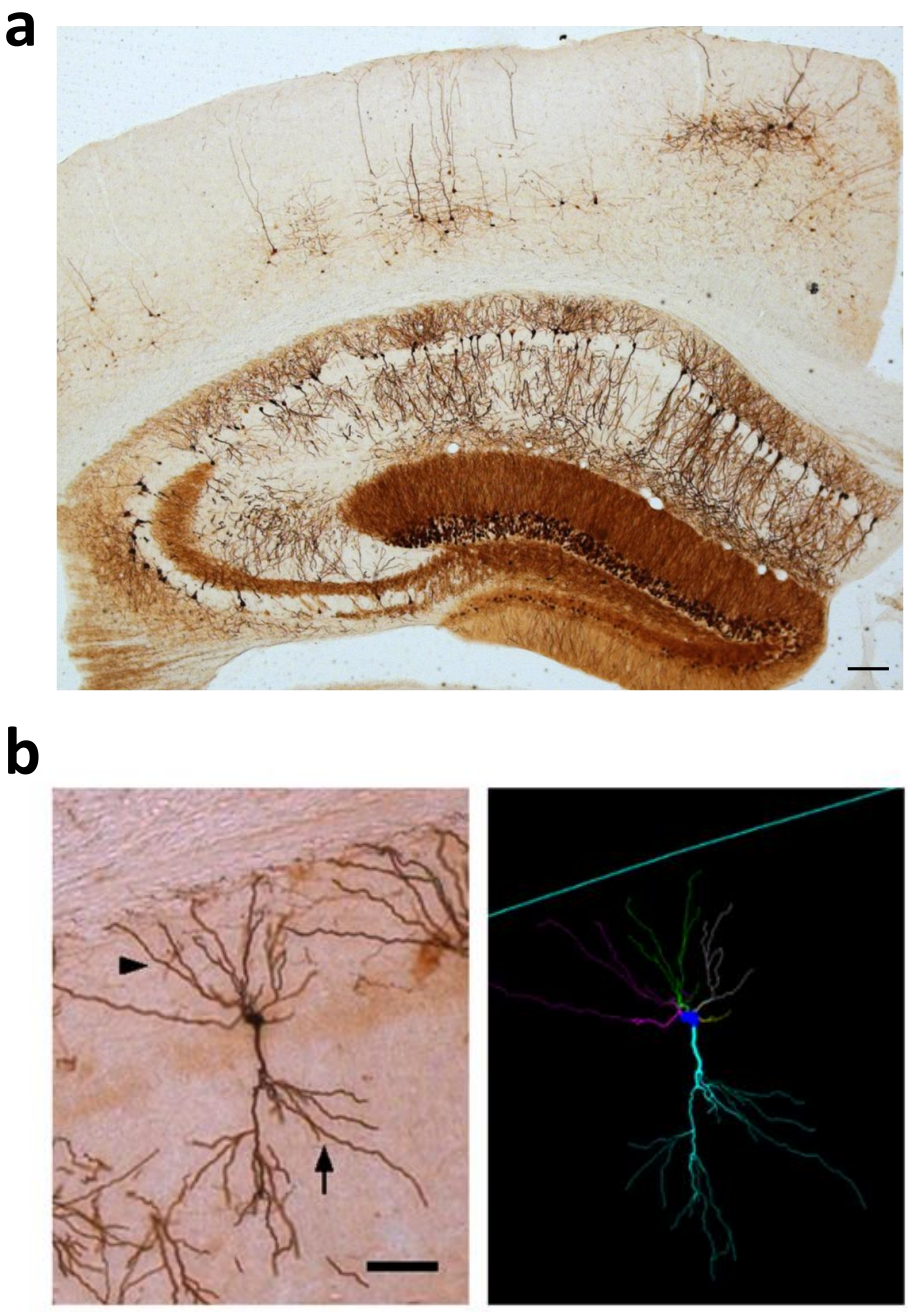

Figure 7. a, GFP immunolabeled hippocampal cells. **b,** CA1 hippocampal neuron (left) and its tracing (right). Arrow indicates apical segment, arrowhead indicates basal segment. Scale Bars: 50µm (a), 50µm (b).

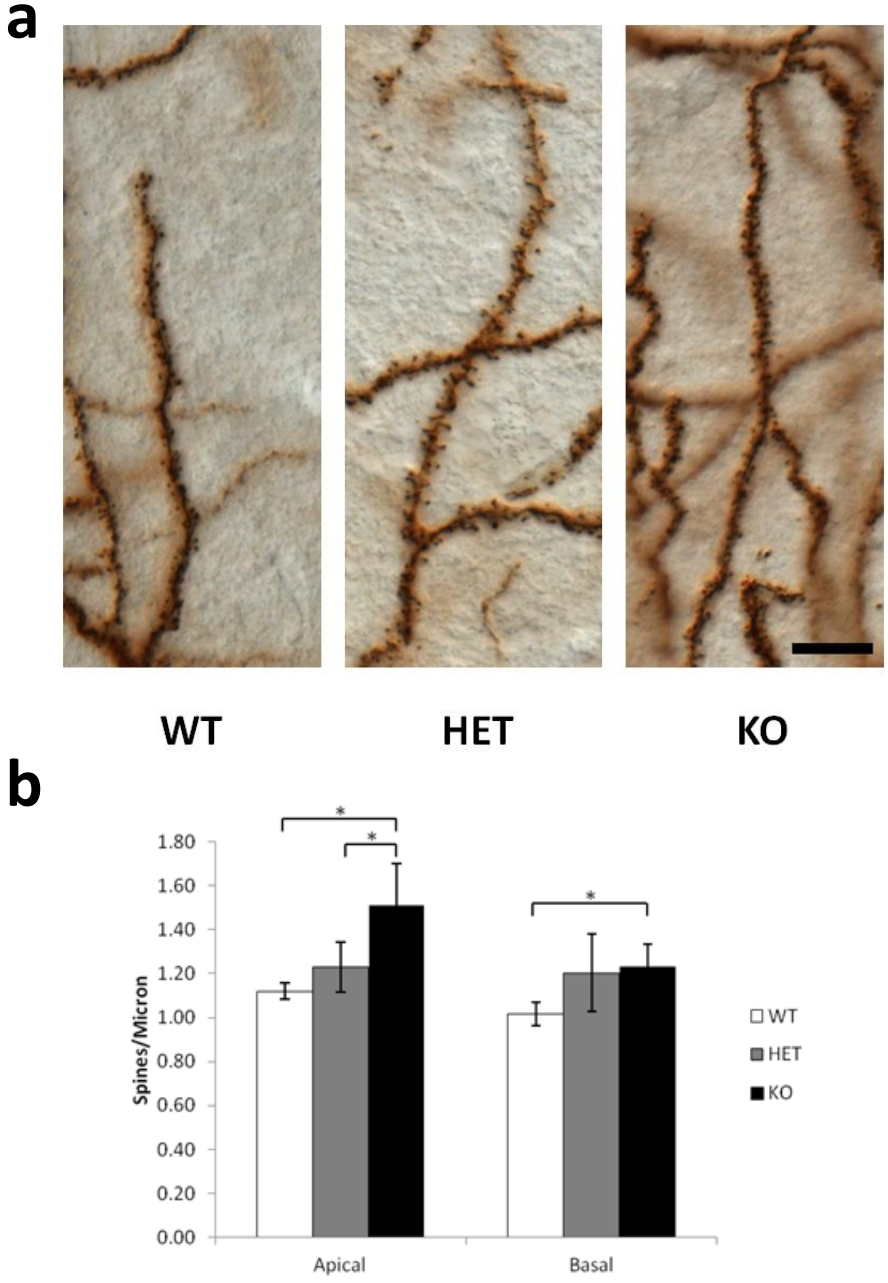

Figure 8. a, Immunolabeled apical segments of CA1 hippocampal neurons. Scale bar: 25µm **b,** Average spine densities in both apical and basal dendrites of WT, HET and *Fmr1* KO mice in CA1 hippocampal neurons of 4 month old mice (mean±s.d.). *indicates $p<0.05$.

Age	Genotype	Region	Branch	Animals (n)	Neurons (n)	Dendritic segments (n)	Protrusions (n)	Total Length of Traced Dendrites (µm)
Layer 5 Pyramidal Neurons								
1 mo	WT	S1BF	Apical	4	12	132	7204	5830.4
1 mo	WT	S1BF	Basal	4	10	142	4907	4438.4
1 mo	KO	S1BF	Apical	3	10	76	5082	4067.9
1 mo	KO	S1BF	Basal	3	10	133	5919	5042.1
4 mo	WT	S1BF	Apical	4	14	112	2667	4569.8
4 mo	WT	S1BF	Basal	4	13	152	2851	4930.6
4 mo	HET	S1BF	Apical	5	17	118	5094	5922.2
4 mo	HET	S1BF	Basal	5	13	126	2337	4074.5
4 mo	KO	S1BF	Apical	5	16	138	5856	6032.9
4 mo	KO	S1BF	Basal	5	12	166	3114	5220.8
4 mo	WT	A1	Apical	5	10	79	2528	3740.2
4 mo	WT	A1	Basal	5	10	114	2765	4399.3
4 mo	HET	A1	Apical	4	10	92	3159	3193.5
4 mo	HET	A1	Basal	4	8	55	1633	2365
4 mo	KO	A1	Apical	3	10	88	3766	3745.9
4 mo	KO	A1	Basal	3	10	118	2596	4265.5
4 mo	WT	V1	Apical	4	10	93	2250	3316.3
4 mo	WT	V1	Basal	4	10	126	2224	3825.7
4 mo	HET	V1	Apical	4	10	65	3046	2707
4 mo	HET	V1	Basal	4	6	66	1447	2153.8
4 mo	KO	V1	Apical	4	10	80	3217	2915.8
4 mo	KO	V1	Basal	4	10	110	2261	3792.9
Layer 2/3 Pyramidal Neurons								
4 mo	WT	S1BF	Apical	4	9	140	5782	4690.1
4 mo	WT	S1BF	Basal	4	9	182	7883	5916.8
4 mo	KO	S1BF	Apical	3	8	133	6280	4656.7
4 mo	KO	S1BF	Basal	3	8	147	6704	5524
CA1 Neurons								
4 mo	WT	CA1	Apical	5	16	99	5981	5355.7
4 mo	WT	CA1	Basal	5	15	99	4926	4887.4
4 mo	HET	CA1	Apical	5	14	77	4731	3828.6
4 mo	HET	CA1	Basal	5	14	90	4008	3337.5
4 mo	KO	CA1	Apical	5	15	73	6199	4110.8
4 mo	KO	CA1	Basal	5	17	109	6298	5041.1

Table 1. Numbers of animals, neurons, dendritic segments, protrusions, and dendritic length quantified for each dendritic compartment, cortical region, genotype, and age examined for each cell type.